Biochemical and Biophysical Research Communications 439 (2013) 378–383

Contents lists available at ScienceDirect

Biochemical and Biophysical Research Communications

journal homepage: www.elsevier.com/locate/ybbrc

Milky spot macrophages remodeled by gastric cancer cells promote peritoneal mesothelial cell injury

Xing-Yu Liu [a,1], Zhi-Feng Miao [a,1], Ting-Ting Zhao [b], Zhen-Ning Wang [a], Ying-Ying Xu [b], Jian Gao [c], Jian-Hua Wu [a], Yi You [a], Hao Xu [a], Hui-Mian Xu [a,*]

[a] Department of Surgical Oncology, The First Affiliated Hospital of China Medical University, Shenyang, Liaoning Province, China
[b] Department of Breast Surgery, The First Affiliated Hospital of China Medical University, Shenyang, Liaoning Province, China
[c] Center of Laboratory Technology and Experimental Medicine, China Medical University, Shenyang, Liaoning Province, China

ARTICLE INFO

Article history:
Received 17 August 2013
Available online 29 August 2013

Keywords:
Peritoneal carcinomatosis
Stomach cancer
Peritoneal macrophage
Human peritoneal mesothelial cell
Transforming growth factor-beta1

ABSTRACT

Peritoneal dissemination (PD) is the most frequent metastatic pattern of advanced gastric cancer (GC) and the main cause of death in GC patients. Human peritoneal mesothelial cell (HPMC) injury induced by gastric cancer cells (GCCs) and GCC outgrowths supported by peritoneal milky spot macrophages (PMSMs) are the key events during gastric cancer peritoneal dissemination (GCPD). In this study, we investigated whether PMSMs remodeled by GCC can induce HPMC injury and create a favorable microenvironment for GCPD. We established a tumor-associated macrophage (TAM) model using *in vitro* cell coculture. Normal macrophages cocultured with GCCs down-regulated expression of antigen-presenting surface molecules CD80, CD86, and MHC-II, but, notably, they up-regulated expression of phagocytic scavenger receptor CD206, which is similar to the M2 macrophage phenotype. In further experiments, various experimental methods were applied to detect the injurious effect of TAMs on HPMCs in another TAM–HPMC coculture. Our results showed that GCCs can induce HPMC apoptosis by unregulated apoptosis associated with cleaved caspase3, cleaved caspase9, and p21 proteins. HPMC growth ceased, and both early- and late-stage apoptosis were observed. Additionally, GCCs can induce HPMC fibrosis via increased expression of epithelial cell marker E-cadherin and decreased expression of mesenchymal cell marker α-SMA. Our results demonstrate that, in the GCPD process, PMSMs were remodeled by GCCs, resulting in phenotypic and functional transformation. In turn, this transformation induced HPMC injury and provided a favorable microenvironment for GCC anchorage and growth. These results may provide new insight into the mechanisms of GCPD.

1. Introduction

Peritoneal dissemination (PD) is one of the most common patterns of metastases in gastric cancer (GC), and it is the main contributor to the failure of radical gastrectomy for advanced gastric carcinoma (AGC) [1,2]. Although the prognosis of patients with gastric cancer peritoneal dissemination (GCPD) seems to have improved as a result of the standardization of surgical techniques and recent advances in intraperitoneal chemotherapies [3,4], the 5-year postoperative survival rate remains low [5]. Moreover, the mechanisms of peritoneal metastasis have not yet been clearly defined.

Human peritoneal mesothelial cells (HPMCs) and peritoneal milky spot macrophages (PMSMs) constitute the first line of defense in the peritoneum. However, when this barrier is breached, the peritoneal microenvironment favors proliferation of GCCs and serves as a rich source of growth factors and chemokines known to be involved in GCPD [6–8]. The monolayer of HPMCs that covers the peritoneum plays an important role in maintaining its structure and function.

In our previous study, gastric cancer cells (GCCs) attached to the integrated HPMC monolayer, and the invasion and migration abilities of GC were effectively inhibited [9,10]. However, a longer period of GCC coculture can induce HMPC apoptosis and fibrosis both by upregulation of caspase3, caspase9, and E-cadherin and by down-regulation of B-cell lymphoma 2 (Bcl-2) and alpha smooth muscle actin (α-SMA). As a result, the HPMC layer collapses and exfoliation takes place. Naked areas of submesothelial connective tissue are thus exposed to the peritoneal cavity, and this peritoneal injury site becomes a favorable microenvironment

* Corresponding author. Address: Department of Surgical Oncology, The First Affiliated Hospital of China Medical University, No. 155 North Nanjing Street, Heping District, Shenyang, Liaoning Province 110001, China. Fax: +86 24 22703576.
E-mail address: fengfeng19998@hotmail.com (H.-M. Xu).
[1] These authors contributed equally to this article.

0006-291X/$ - see front matter © 2013 Elsevier Inc. All rights reserved.
http://dx.doi.org/10.1016/j.bbrc.2013.08.073

for GCPD. Therefore, the structure and function of HPMCs play roles in preventing the adhesion and colonization of cancer cells [7,11,12]. HPMC injury induced by apoptotic and fibrotic cytokines is the key event in GCPD.

Peritoneal milky spots (PMSs) are widely located in mammalian peritonea, which are mainly composed of immature macrophages and natural killer cells, as well as a few antigen-presenting dendritic cells and B cells [13,14]. Tumor cells enter PMSs as they exfoliate from primary tumor lesions, colonize within them, and form micrometastases, thus inducing PD. Immature peritoneal milky spot macrophages (PMSMs) lack antigen-presenting and tumor-eradicating abilities; they cannot effectively scavenge tumor cells [15]. Conversely, PMSMs remodeled by tumor cells form tumor-associated macrophages (TAMs) with an alternative active macrophages (M2 macrophages) phenotype, which provide nutrition and support for tumor cells. Therefore, PMSM remodeling is another key event during PD [16].

Presently, the source of apoptotic and fibrotic cytokines that induce HPMC injury within the GCPD microenvironment is mainly thought to be peritoneum-free GCC [6–13]. However, in the GCPD process, many inflammatory cells are infiltrated within the PMS chemotaxis by GCCs from peripheral blood or nearby PMSs. These inflammatory cells are mainly composed of M2 PMSMs. In turn, this induces a chronic inflammatory microenvironment in which large quantities of stroma remolding factors, such as transforming growth factor beta 1 (TGF-β1) and connective tissue growth factor (CTGF), are released [17–19]. TGF-β1 is the most potent apoptotic and fibrotic stimuli released by GCCs, so we hypothesized that PMSM remodeling by GCCs induces HPMC injury and creates a microenvironment favorable to peritoneal metastasis. In this study, we investigated the interaction of TAMs and HPMCs at the early stage of GCPD, and we have formulated new explanation for HPMC injury during GCPD.

2. Materials and methods

2.1. Reagents and antibodies

RPMI-1640, Dulbecco's modified Eagle medium (DMEM) and fetal bovine serum (FBS) were purchased from Hyclone (Logan, UT, USA). Cell culture materials were purchased from Corning (Corning, NY, USA); diamidino-2-phenylindole (DAPI) phorbol-12-myristate 13-acetate (PMA), 3-(4,5-dimethylthiazol-2-yl)-2,5-diphenyltetrazolium bromide (MTT) and rabbit anti-human fibronectin antibodies were purchased from Sigma–Aldrich (St. Louis, MO, USA). Mouse anti-human CD80-fluorescein isothiocyanate (FITC), mouse anti-human CD86-FITC, mouse anti-human MHC-II-FITC, mouse anti-human CD206-FITC, mouse anti-human E-cad antibodies, and an Annexin V-PI apoptosis detection kit were purchased from Becton Dickinson (San Jose, CA, USA). A Quantikine human TGF-β1 ELISA kit was purchased from R&D Systems (Minneapolis, MN, USA). Mouse anti-human CD68, mouse anti-human CD163, mouse anti-human CK-8, and rabbit anti-human α-SMA antibodies were purchased from Abcam (Cambridge, MA, USA). β-actin and secondary antibodies were purchased from Santa Cruz Biotechnology (Santa Cruz, CA, USA). E-caprolactone (ECL) solution was purchased from Pierce Chemical Co. (Rockford, IL, USA). Fluorescence secondary antibody was purchased from Invitrogen (Carlsbad, CA, USA).

2.2. Cell lines

The HPMC cell line HMR-SV5, human monocyto-macrophage line THP-1, human normal gastric glandular epithelial cell line GES-1, and the poorly differentiated GCC line SGC-7901 were purchased from the cell bank of the Chinese Academy of Sciences (Shanghai, China). SGC-7901 was cultured in DMEM medium containing 10% FBS. The HMR-SV5, THP-1, GES-1 cell lines were all cultured in RPMI-1640 media containing 10% FBS. All cell cultures were incubated continuously under a 5% CO_2 atmosphere at 37 °C.

2.3. Establishment of the TAM model

THP-1 cells ($\sim 1 \times 10^6$ cells/well) were inoculated with 50 μg/ml PMA; culture media were changed when THP-1 growth attached to the plastic substrates. Following attachment, a coculture insert was added, and approximately 2×10^5 GES-1 or SGC-7901 cells were plated into the upper chamber, respectively. The whole coculture system was cultured in RPMI-1640 containing 10% FBS for 72 h. THP-1 in the lower chamber was collected after coculture for cell-surface staining analysis, western blot assay, and immunofluorescence assay. THP-1 cells cocultured with GES-1 cells were referred to as the normal macrophage group (T group); THP-1 cells cocultured with SGC-7901 cells were referred to as the TAMs group (TA group).

2.4. Establishment of TAM-induced HPMC injury model

HMR-SV5 cells ($\sim 1 \times 10^6$) were inoculated into a six-well cell culture plate until 80% cell fusion, at which point a cocultured insert was added. For both the T and TA groups, approximately 2×10^5 THP-1 cells were plated into the upper chamber, then the whole coculture system was cultured in RPMI-1640 containing 10% FBS for 48 h. The cells in the upper chamber were then discarded, and the HMR–SV5 cells in the lower chamber were collected for MTT assay, western blot assay, and immunofluorescence assay. Normal untreated SV5 cells were referred to as the SV5-C group; cells cocultured with T group macrophages were referred to as the SV5-T group; and TA group macrophages and were referred to as the SV5-TA group.

2.5. Scanning electron microscopic (SEM) detection

Cell specimens were placed on a cover slip, and glutaraldehyde-sodium cacodylate fixative fluid was added to the specimens and allowed to adhere for 2–3 h. The specimens were washed twice with sodium cacodylate buffer, followed directly by gradient dehydration in ethanol. Then the specimens were transferred into 100% isopentyl acetate and dried to a critical point. Then the specimens were coated with gold in a vacuum and prepared for examination in the scanning electron microscope (JCM 5000, Nikon, Japan) .

2.6. Cell surface antigen analysis by fluorescence activated cell sorting (FACS)

Macrophages from each group were harvested using trypsin–EDTA then washed twice with ice-cold phosphate buffering solution (PBS) with 1% bovine serum albumin (BSA). Incubation was carried out, respectively, with CD80-FITC, CD86-FITC, MHC-II-FITC, CD206-FITC antibodies for 30 min at 4 °C in the dark. After washing twice with ice-cold PBS with 1% BSA, cell-surface staining was then determined by flow cytometry (FACS Caliber, Becton Dickinson).

2.7. Cytokine assay by ELISA

Cytokine production was determined using a Quantikine human TGF-β1 ELISA kit (R&D Systems) according to the manufacturer's instructions.

2.8. MTT detection

HPMC variability was assessed using an MTT [3-(4,5-dimethylthiazol-2-yl)-2,5-diphenyltrazoliumbromide] assay. Approximately 1×10^4 cells/well cocultured with HPMCs were seeded into 96-well culture plates and cultured in DMEM with 10% FBS for 12–72 h. Then, cells were incubated with 20 μL MTT (10 mg/ml) for 4 h at 37 °C, and 200 μL DMSO was pipetted to solubilize the formazan product for 20 min at room temperature. The optical density (OD) was determined using a spectrophotometer (Bio-800, Bio-Rad, Berkeley, CA, USA) at a wavelength of 570 nm. Approximately 1×10^4 cells/well of untreated HPMCs were cultured with serum-free DMEM medium as a control group.

2.9. Detection of apoptosis by annexin v-PI cell-surface staining

Apoptosis of HMR-SV5 was detected using an annexin V-propidium iodide apoptosis detection kit (Becton Dickinson) according to the manufacturer's instructions. Briefly, cells were resuspended in 1× binding buffer at a concentration of 1×10^6/ml. Then 5 μL annexin V-FITC antibody and 5 μL PI were added in the dark at room temperature for 15 min. After washing twice with 1× binding buffer, cell-surface staining was analyzed by flow cytometry (FACS Caliber, Becton Dickinson). HPMCs in the upper-right quadrant and the lower-right quadrant showed late-stage and early-stage apoptosis, respectively.

2.10. Western blotting

Cells were washed twice with cold PBS and were collected with a cell scraper. Then 50 μL radio immunoprecipitation assay (RIPA) buffer and 1 mM phenylmethanesulfonyl fluoride (PMSF), 1 μg/ml leupeptin, 1 mM β-glycerrophosphate, 2.5 mM sodium pyrophosphate, and 1 mM Na_3VO_4 were added, followed by incubation on ice for 20 min and centrifugation at 12,000g for 20 min at 4 °C. The supernatant was then transferred to a new Eppendorf tube to test protein concentration. Protein samples (50 μg) were resolved with 10% sodium dodecyl sulfate (SDS) polyacrylamide gel then transferred to a polyvinylidene difluoride (PVDF) membrane and blocked in 10% BSA solution for 2 h at room temperature. After washing, the membrane was incubated with specific antibodies at the proper concentration in Tris-buffered saline with Tween (TBST) solution overnight at 4 °C. After washing the membrane three times for 15 min with TBST solution, the membrane was further incubated with horseradish peroxidase (HRP)-conjugated secondary antibodies in TBST solution for 2 h at room temperature. The membrane was then washed three times for 15 min with TBST solution and was then incubated with ECL solution for 1 min. Protein bands were visualized using ECL chemiluminescence.

2.11. Cell immunofluorescence confocal imaging

Cells were fixed in 4% paraformaldehyde in 20 mM HEPES (pH 7.4) for 20 min, rinsed three times, and incubated with primary antibodies for 1 h at room temperature. The membrane was then rinsed three times and incubated with Alexa Fluor-conjugated secondary antibody for 30 min at room temperature in the dark. DAPI was used for nuclear counterstaining. The stained cells were mounted and viewed under an immunofluorescence microscope (FV1000, Olympus, Japan).

2.12. Statistical analysis

All statistical analyses were performed using SPSS version 16.0 software (SPSS, Inc., Chicago, IL, USA). Data obtained from three or more separate experiments are expressed as mean ± SD. ANOVA was used for the statistical analysis of data and calculation of p values. Statistical significance was set at $p < 0.05$.

3. Results

3.1. TAMs model established by THP-1 and SGC7901 coculture

The morphology of the macrophages and SEM images showed a larger volume of macrophages in the T group than in the TA group. Cell folding abounded in the T group, and the number and the length of pseudopodia increased in the T group (Fig. 1A).

The expressions of macrophage surface antigens in the two groups were detected by flow cytometry (Fig. 1B). The expression of M1 macrophage surface antigens in the TA group was notably down-regulated. The expression of CD80 was down-regulated from 20.43% to 5.03%; the expression of CD86 was down-regulated from 35.82% to 24.02%; and the expression of MHC-II was down-regulated and from 8.69% to 3.54%. The expression of M2 macrophage surface antigens CD206 was up-regulated from 1.04% to 4.22%. After 72 h coculture, cell immunofluorescence confocal imaging of macrophage cocultured with SGC7901 showed elevated expression of M2 macrophage marker CD163 compared with macrophage cocultured with GES-1 (Fig. 1C). But this coculture did not affect the expression of the normal macrophage marker CD68. TGF-β1 expression in both the T and the TA groups macrophage and SGC7901 was determined by ELISA (Fig. 1D). Macrophage expression of TGF-β1 in the TA group was much higher compared with the T group (1062.1 ± 102.1 pg/ml vs. 96.3 ± 8 pg/ml; $P < 0.05$). As described previously, GCC-induced HPMC injury is caused by a high level of expression of TGF-β1 [7,10,11]. We also compared TGF-β1 expression between the TA group macrophage and the GCC line SGC7901. Our results showed that the TA group macrophage expressed an even higher TGF-β1 level (1062.1 ± 102.1 pg/ml vs. 571.3 ± 57.4 pg/ml; $P < 0.05$).

3.2. TAMs induced HPMC apoptosis in a time-dependent manner

The expressions of proteins related to apoptosis were analyzed by western blotting assay (Fig. 2A). After 48 h coculture, expressions of apoptosis-related proteins caspase3, caspase9, and p21 in the SV5-TA group were elevated compared with those of the other two groups. The results of an MTT assay indicated that proliferation of HPMCs in the SV5-TA group ceased after they were cocultured with TAMs; however, HPMCs in both the SV5-T and SV5-C groups displayed normal cell proliferation. Cell proliferation was calculated using the following equation:

Cell proliferation rate (%) = OD (Experimental group−Control group)/OD control group × 100%

where OD is optical density. The cell proliferation rates in the three groups at 48 h were as follows: SV5-C 92.1 ± 7.6%; SV5-T, 112.4 ± 9.3%; and SV5-TA 7.4 ± 1.4% (Fig. 2B). The apoptotic tendency in the SV5-TA group became more obvious when the period of coculture was extended. The apoptosis of HPMCs in each group was tested by annexin V-PI double staining (Fig. 2C). Apoptosis of HPMCs in the SV5-TA group became more notable after 48 h of coculture. The apoptosis rates of the three groups were as follows: SV5-C, 2.3% (early stage) and 4.61% (late stage); SV5-T, 1.9% (early stage) and 3.04%; and SV5-TA, 7.4% (early stage) and 38.57% (late stage).

3.3. TAMs induced HPMC fibroblastic transformation

The expressions of proteins related to fibroblastic transformation in each group were detected by western blotting. HPMCs in the SV5-C and SV5-T groups displayed high expression of epithelial cell-related proteins E-cad and CK-8 and low expression of

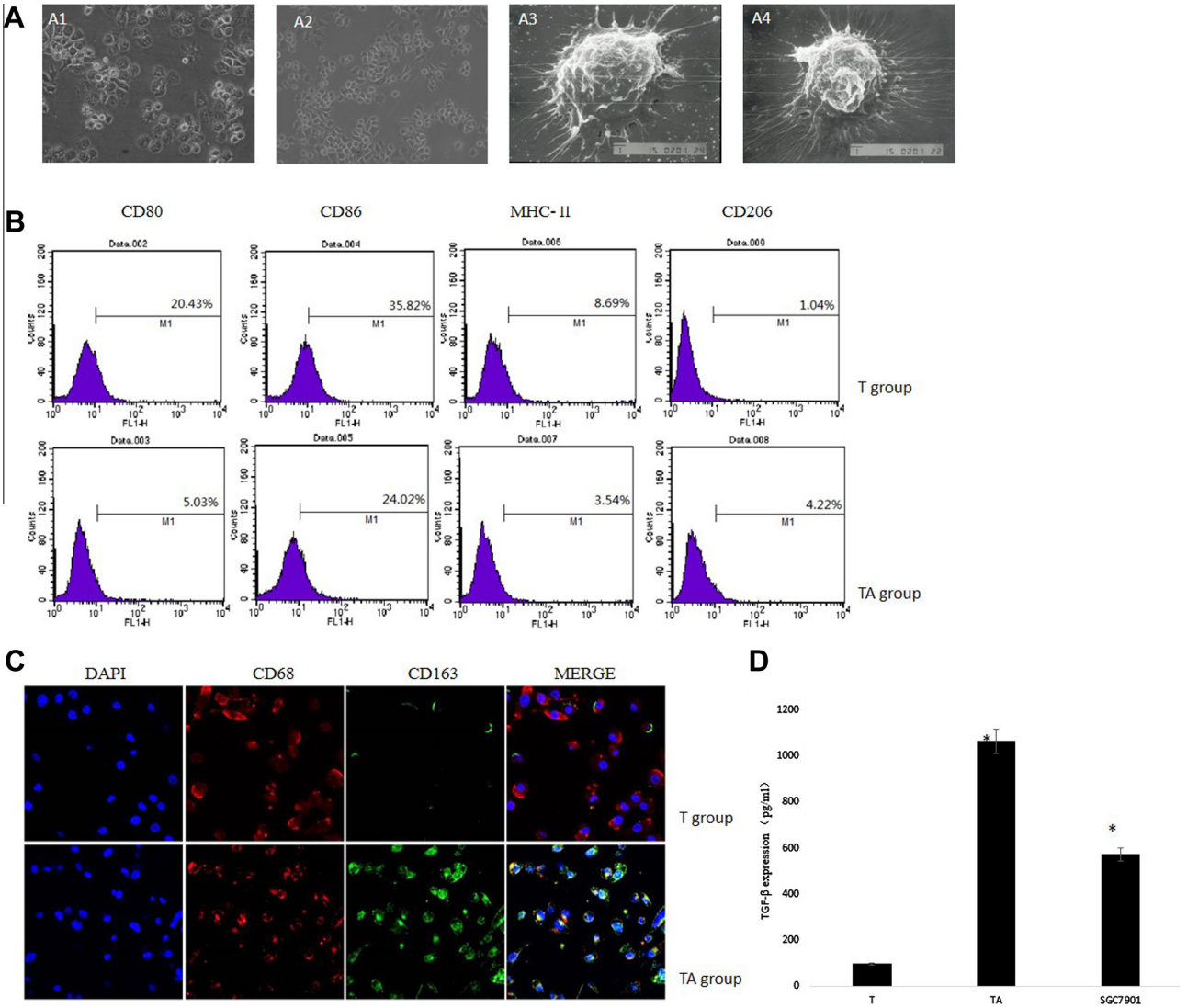

Fig. 1. TAM model established by THP-1 and SGC7901 coculture (A) Morphology changes of macrophages in both the T group (A1, A3) and the TA group (A2, A4) by a phase contrast of microphages (A1, A2) and scanning electron microscopy (A3, A4) (60×). (B) Flow cytometric analyses of the surface expression of CD80, CD86, and MHC-II in the T and TA groups. Macrophages were incubated with CD80-FITC, CD86-FITC, and MHC-II-FITC antibodies for 30 min at 4 °C in the dark. After washing twice in ice-cold PBS with 1% BSA, surface staining was analyzed by flow cytometry. (C) Immunofluorescence analysis of macrophage-related protein expression in the T and TA groups. CD68 shows red staining; CD163 shows green staining, DAPI shows blue staining (60×). (D) TGF-β1 levels in the conditioned media of the T and TA groups were determined by ELISA. Results are expressed as pg /ml/1 × 10^5 cells (mean ± SD, $n = 3$, $^*P < 0.05$). For interpretation of the references to colour in this figure legend, the reader is referred to the web version of this article.

mesenchymal-related proteins α-SMA and FN. However, HPMCs in the SV5-C group after 48 h of coculture with TAMs showed increased FN expression and decreased E-cad and CK-8 expression (Fig. 3A). Cell immunofluorescence confocal imaging (Fig. 3B) showed that HPMCs in the SV5-C and SV5-T groups exhibited the typical polygonal and cobblestone-like morphologies with integrated expression of E-cad in the cell membrane and very low expression of α-SMA. However, in the SV5-TA group, HPMCs underwent significant morphological change: cells were spindle-like with reduced cytoplasm volume, E-cad expression was interrupted, and α-SMA expression was obviously upregulated.

4. Discussion

The "seed and soil" theory suggests that malignant tumor metastasis is a result of the cascade development of special tumor cell clones (seeds) in a suitable microenvironment (soil) [20]. The results of previous studies have indicated that, after exfoliated GCCs enter the abdominal cavity, HPMCs are directly acted upon by GCCs, which in turn undergo fibrotic transformation. The fibroblast-transformed HPMCs then induce an enhanced effect of chemotaxis and adhesion on GCCs, which results in GCPD [10–13]. Meanwhile, GCCs have also been shown to induce HPMC apoptosis, which leads to subcutaneous matrix exposure, forming an apterium in which GCCs then enter and implant, thus precipitating GCPD [21]. This cascade is mainly mediated by the TGF-β1 pathway [12,13,21].

In other studies, another pattern of GCPD has been considered to indicate that free cancer cells in the peritoneal cavity prefer to colonize in peritoneal milky spots (PMS), thereby forming metastatic nodules [11,22–24]. PMSMs located within these nodules are remodulated by GCCs, supporting the outgrowth of GCCs and creating a microenvironment of chronic inflammation that is favorable to GCPD.

In this study, we sought to determine whether TAMs can induce injury and thus create a favorable microenvironment for GCPD,

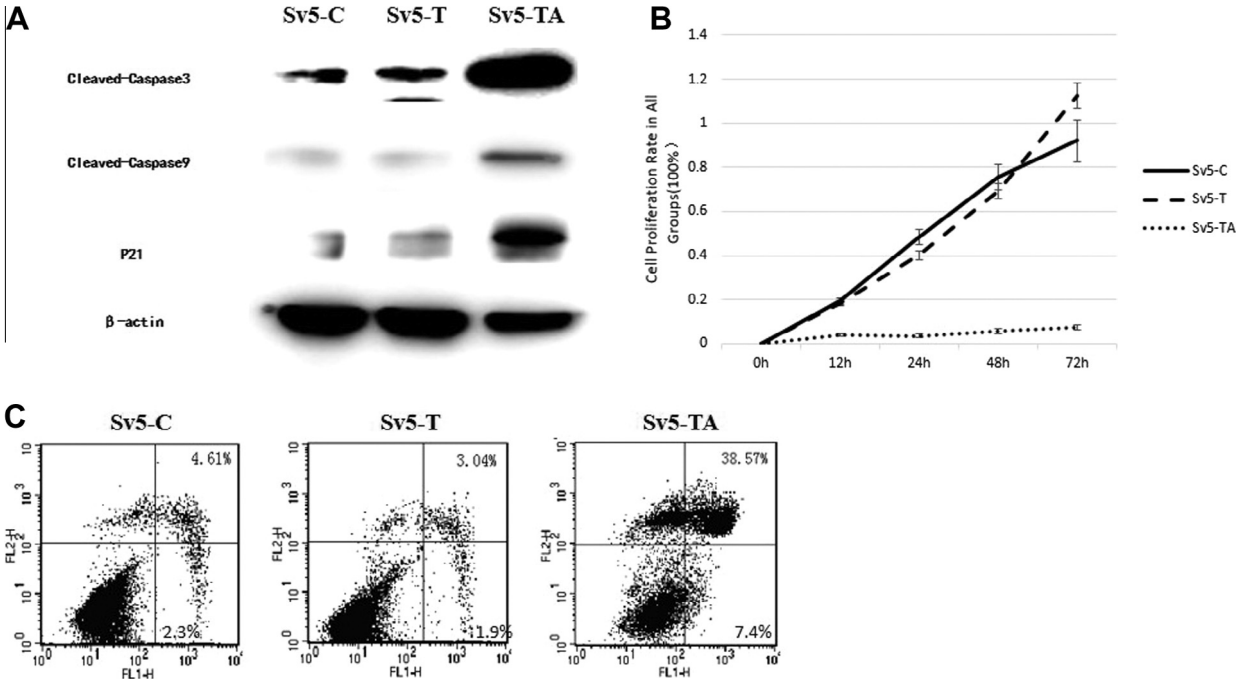

Fig. 2. TAMs induce HPMC apoptosis in a time-dependent manner (A) Western blot showing the expression of apoptosis-related caspase3, caspase9, and p21 protein in the Sv5-C, Sv5-T, and Sv5-TA groups. β-actin served as protein-loading control. (B) The MTT assay shows variability of HPMC in the Sv5-C, Sv5-T, and Sv5-TA groups. Data are expressed as a fold change relative to control (non-treated Sv5). Values are given as the mean ± SD of three experiments. (C) Annexin V-PI double staining shows early stage apoptosis of HPMC in the Sv5-C, Sv5-T, and Sv5-TA groups.

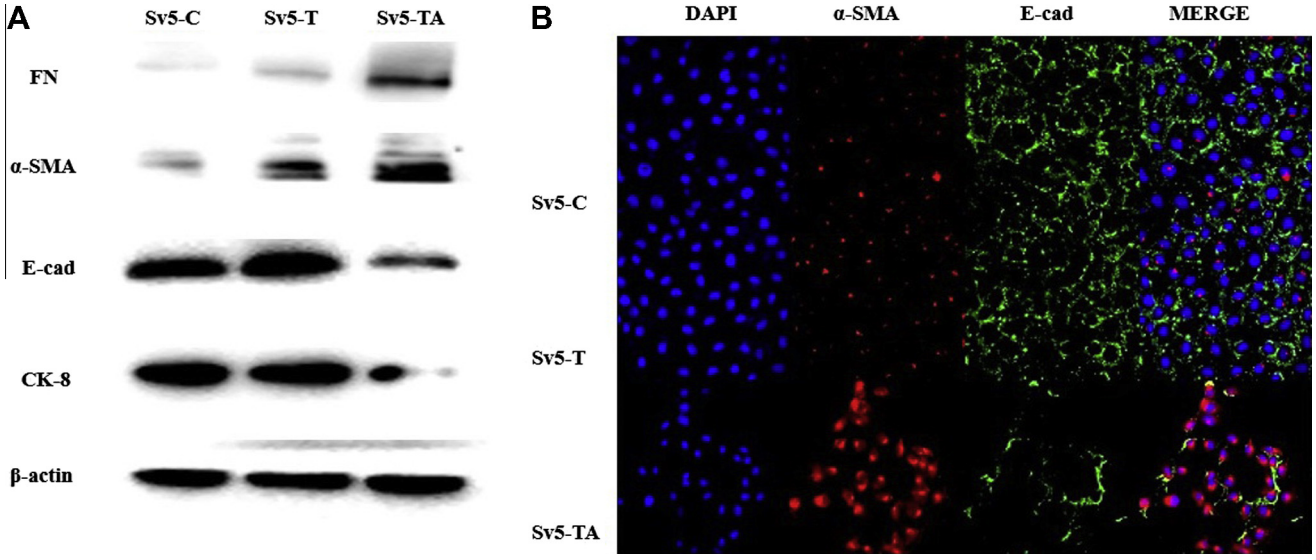

Fig. 3. TAMs induce HPMC fibroblastic transformation (A) Western blot showing the expression of EMT-related FN, α-SMA, E-cad, CK-8 protein in the SV5-C, SV5-T, and SV5-TA groups. β-actin served as the protein-loading control. (B) Immunofluorescence analysis of EMT-related protein expression in the SV5-C, SV5-T, and SV5-TA groups. E-cadherin shows green staining; a-SMA shows red staining, DAPI shows blue staining (60×). For interpretation of the references to colour in this figure legend, the reader is referred to the web version of this article.

considering two modes of GCPD discussed above. First, we established a TAM model using *in vitro* cell coculture. After normal macrophages were cocultured with GCC, the expressions of the antigen-presenting surface antigens CD80, CD86, and MHC-II were notably down-regulated, but the expression of phagocytic scavenger receptor CD206 was notably up-regulated. Meanwhile, the expression of M2 phenotypic protein CD163, which is closely related to TAMs in terms of phenotype and function, was also notably up-regulated. In further experiments, the TAM model was used to coculture normal human peritoneal HPMCs, and various laboratory analyses were conducted to detect the injurious effect of TAMs on HPMCs. The injurious effect of TAMS on HPMCs mainly presented in two aspects: First, TAMs notably inhibited the growth and induced the apoptosis of normal HPMCs. Second, TAMs induced normal cells to undergo fibrotic transformation. The expressions of epithelial proteins E-cad and CK-8 were notably down-regulated, whereas the expressions of mesenchymal proteins α-SMA and FN were notably up-regulated.

Plasticity is a hallmark characteristic of the macrophage. In general, two forms of macrophages, activated (M1) and polarized (M2), which mirror T-helper type 1 (Th1) and T-helper type 2 (Th2) definitions of cell-mediated immunity. Classically activated

macrophages (M1) are described as pro-inflammatory, with tumor-resistant effects. In contrast, alternatively activated, or polarized, macrophages (M2) are more prone to immunoregulation, stoma-remodeling, and pro-tumoral activities [17–19]. In fibrotic diseases such as hypertension, pulmonary fibrosis, and hepatic cirrhosis, in which chronic inflammation accounts for the basic pathological changes, M2 macrophages abound in foci, accompanied by myofibroblast hyperplasia. The main sources of myofibroblasts are epithelial cells (e.g., vascular endothelial cells, alveolar epithelial cells, etc.), which are produced by epithelial-mesenchymal transformation (EMT) [25,26]. These epithelial cells are similar to HPMCs in foci. The TGF-β1 expressed in M2 macrophages plays a key role in the EMT process [27]. Therefore, a chronic inflammatory microenvironment, caused by M2 macrophage infiltration, is also considered to be one of the main induced factors in epithelial cells undergoing fibrotic transformation in foci. Because M2 macrophages abound in the foci of peritoneal metastases at the early stage of GC, we hypothesize that GCCs enter into milky spots and act on macrophages, which in turn transform phenotypically and functionally. The remodeled macrophages (i.e., TAMs) directly enhance the invasive ability of GCCs and further degrade the integrity of HPMCs by inducing injury, enhancing the opportunity for adhesion and colonization by GCCs.

Our experimental results indicate that, in the process of GCPD, PMSMs are reeducated by GCCs, resulting in phenotypic and functional transformation. The reeducated macrophages induce HPMC apoptosis and fibrosis transformation, resulting in sub-HPMC collagen exposure and remodeled peritoneum stroma, which, in turn, create a favorable "soil" for the anchorage-dependent growth of GCCs.

References

[1] G. Glockzin, P. Piso, Current status and future directions in gastric cancer with peritoneal dissemination, Surg. Oncol. Clin. N. Am. 21 (4) (2012) 625–633.

[2] J.H. Li, S.W. Zhang, J. Liu, et al., Review of clinical investigation on recurrence of gastric cancer following curative resection, Chin. Med. J. (Engl) 125 (8) (2012) 1479–1495.

[3] Z. Lu, J. Wang, M.G. Wientjes, et al., Intraperitoneal therapy for peritoneal cancer, Future Oncol. 6 (10) (2010) 1625–1641.

[4] Y. Yonemura, Y. Endou, T. Sasaki, et al., Surgical treatment for peritoneal carcinomatosis from gastric cancer, Eur. J. Surg. Oncol. 36 (12) (2010) 1131–1138.

[5] I. Thomassen, Y.R. van Gestel, B. van Ramshorst, et al., Peritoneal carcinomatosis of gastric origin: A population-based study on incidence, survival and risk factors, Int. J. Cancer (2013). Jul 5.

[6] C.G. Jiang, L. Lv, F.R. Liu, et al., Connective tissue growth factor is a positive regulator of epithelial-mesenchymal transition and promotes the adhesion with gastric cancer cells in human peritoneal mesothelial cells, Cytokine 61 (1) (2013) 173–180.

[7] D. Na, Z.D. Lv, F.N. Liu, et al., Gastric cancer cell supernatant causes apoptosis and fibrosis in the peritoneal tissues and results in an environment favorable to peritoneal metastases, *in vitro* and *in vivo*, BMC Gastroenterol. (12) (2012) 34, http://dx.doi.org/10.1186/1471-230X-12-34.

[8] Z. Li, Z. Miao, G. Jin, et al., βig-h3 supports gastric cancer cell adhesion, migration and proliferation in peritoneal carcinomatosis, Mol. Med. Rep. 6 (3) (2012) 558–564.

[9] Z.D. Lv, D. Na, X.Y. Ma, et al., Human peritoneal mesothelial cell transformation into myofibroblasts in response to TGF-β1 *in vitro*, Int. J. Mol. Med. 27 (2) (2011) 187–193.

[10] D. Na, Z.D. Lv, F.N. Liu, et al., Transforming growth factor beta1 produced in autocrine/paracrine manner affects the morphology and function of mesothelial cells and promotes peritoneal carcinomatosis, Int. J. Mol. Med. 26 (3) (2010) 325–332.

[11] M. Shimomura, T. Hinoi, S. Ikeda, T. Adachi, et al., Preservation of peritoneal fibrinolysis owing to decreased transcription of plasminogen activator inhibitor-1 in peritoneal mesothelial cells suppresses postoperative adhesion formation in laparoscopic surgery, Surgery 153 (3) (2013) 344–356.

[12] T. Tsukada, S. Fushida, S. Harada, et al., The role of human peritoneal mesothelial cells in the fibrosis and progression of gastric cancer, Int. J. Oncol. 41 (2) (2012) 476–482.

[13] J. Rangel-Moreno, J.E. Moyron-Quiroz, D.M. Carragher, et al., Omental milky spots develop in the absence of lymphoid tissue-inducer cells and support B and T cell responses to peritoneal antigens, Immunity 30 (5) (2009) 731–743.

[14] S. Wilkosz, G. Ireland, N. Khwaja, et al., A comparative study of the structure of human and murine greater omentum, Anat. Embryol. (Berl) 209 (3) (2005) 251–261.

[15] S.J. Oosterling, G.J. van der Bij, M. Bögels, et al., Insufficient ability of omental milky spots to prevent peritoneal tumor outgrowth supports omentectomy in minimal residual disease, Cancer Immunol. Immunother. 55 (9) (2006) 1043–1051.

[16] A.M. Lopes Cardozo, A. Gupta, M.J. Koppe, et al., Metastatic pattern of CC531 colon carcinoma cells in the abdominal cavity: an experimental model of peritoneal carcinomatosis in rats, Eur. J. Surg. Oncol. 27 (4) (2001) 359–363.

[17] G. Solinas, G. Germano, A. Mantovani, et al., Tumor-associated macrophages (TAM) as major players of the cancer-related inflammation, J. Leukoc. Biol. 86 (5) (2009) 1065–1073.

[18] A. Sica, Role of tumour-associated macrophages in cancer-related inflammation, Exp. Oncol. 32 (3) (2010) 153–158.

[19] K.S. Siveen, G. Kuttan, Role of macrophages in tumour progression, Immunol. Lett. 123 (2) (2009) 97–102.

[20] D. Jayne, Molecular biology of peritoneal carcinomatosis, Cancer Treat. Res. 134 (2007) 21–33.

[21] D. Na, F. Liu, Z. Miao, et al., Destruction of gastric cancer cells to mesothelial cells by apoptosis in the early peritoneal metastasis, J. Huazhong Univ. Sci. Technolog. Med. Sci. 29 (2) (2009) 163–168.

[22] S.M. Khan, H.M. Funk, S. Thiolloy, et al., *In vitro* metastatic colonization of human ovarian cancer cells to the omentum, Clin. Exp. Metastasis 27 (3) (2010) 185–196.

[23] L. Cao, X. Hu, Y. Zhang, et al., Omental milky spots in screening gastric cancer stem cells, Neoplasma 58 (1) (2011) 20–26.

[24] E.W. Sorensen, S.A. Gerber, A.L. Sedlacek, et al., Omental immune aggregates and tumor metastasis within the peritoneal cavity, Immunol. Res. 45 (2–3) (2009) 185–194.

[25] B. Gao, E. Seki, D.A. Brenner, et al., Innate immunity in alcoholic liver disease, Am. J. Physiol. Gastrointest. Liver Physiol. 300 (4) (2011) G516–525.

[26] T.A. Wynn, Integrating mechanisms of pulmonary fibrosis, J. Exp. Med. 208 (7) (2011) 1339–1350.

[27] T.J. Standiford, R. Kuick, U. Bhan, et al., TGF-β-induced IRAK-M expression in tumor-associated macrophages regulates lung tumor growth, Oncogene 30 (21) (2011) 2475–2484.